Cation Migration upon Adsorption of Methanol in NaY and NaX Faujasite Systems: A Molecular Dynamics Approach

G. Maurin,*,† D. F. Plant,†,‡ F. Henn,† and Robert G. Bell*,‡

Laboratoire LPMC, UMR CNRS 5617, Université Montpellier II, Pl. E. Bataillon, 34095 Montpellier Cedex 05, France, and Davy Faraday Research Laboratory, Royal Institution of Great Britain, 21 Albemarle Street, London W1S 4BS, United Kingdom

Received: April 3, 2006; In Final Form: July 11, 2006

Molecular dynamics simulations have been carried out to address the question of cation migration upon adsorption of methanol in NaY and NaX faujasite systems as a function of the loading. For NaY, it has been shown that, at low and intermediate loadings, SII cations can migrate toward the center of the supercage due to strong interactions with the adsorbates, followed by a hopping of SI′ from the sodalite cage into the supercage to fill the vacant SII site. A SI′ cation can also migrate across the double six ring and takes a SI′ vacant position. SI cations mainly remain trapped in their initial sites whatever the loading. At high loading, only limited motions are observed for SII cations due to steric effects induced by the presence of adsorbates within the supercage. For NaX, the SIII′ cations which occupy the most accessible adsorption sites are significantly moving upon coordination to the methanol molecules; the extent of this mobility exhibits a maximum for 48 methanol molecules per unit cell before decreasing at higher loadings due to steric hindrance. In addition, the SI′ and SII cations remain almost trapped in their initial sites whatever the loading. Indeed, the most probable migration mechanism involves SIII′ cation displacements into nearby SIII′ sites.

1. Introduction

Due to their unique characteristics, zeolites are involved in a large domain of chemical science and technology including catalytic and separation processes, storage of adsorbed molecules, and ion exchange.[1,2] Many research efforts performed both experimentally and theoretically have been thus focused on this class of materials not only because of their technological importance but also because they represent model systems for a wide range of investigations, including the structural properties of the framework and the static or dynamic behavior of various adsorbates in their confined geometries.[3] The aluminosilicate framework of zeolites is characterized by pore systems consisting of channels and cages. The anionic character of the lattice due to the substitution of silicon by aluminum is neutralized by the presence of exchangeable cations which are located in well-defined surface sites surrounded by the oxygen atoms of the framework.[4] Knowledge of the location and distribution of extraframework cation is a crucial point because it influences the distribution of the electron density in the framework[5] and hence the interactions with the adsorbed molecules, leading to possible changes in the adsorption, separation, and catalytic properties of the cation-exchanged zeolites. It was already reported that the nature and positions of the cations which control the electrostatic field within the zeolite cages can strongly modify the adsorption and reactivity of the adsorbate molecules.[6,7] Recent research effort has been devoted to the migration of extraframework cations when adsorbing or desorbing water molecules.[8−15] We previously reported a redistribution of the cation in the Na−mordenite zeolite system upon water adsorption by combining dielectric relaxation spectroscopy and energy minimization techniques.[8] Similar behavior has also been reported in different zeolite systems including faujasite,[9−13] 4A,[14] and natrolite,[15] using experimental techniques and modeling approaches based on molecular dynamics and Monte Carlo simulations. In NaY faujasite systems, the SI−SI′ cation redistribution was predicted, following a direct cation−water interaction within the sodalite cages, whereas SII cations surprisingly do not redistribute upon water adsorption.[10] More recently, it was established that cation redistribution can occur in dry zeolite−adsorbate systems, leading to possible changes in the adsorption properties due to the increasing accessibility of the cation adsorption sites. Previous studies, both experimental and computational, have focused on the adsorption of halocarbons in faujasite systems.[5,16−20] Neutron scattering and X-ray diffraction studies have suggested that the SI′ cations in the sodalite cages migrate into the supercages upon adsorption of both CHF_2CHF_2[16] and $CFCl_3$.[18] Similar findings were reported by Sanchez-Sanchez et al. using MAS NMR spectroscopy, indicating possible motion of the sodium ions upon $CHCl_3$ adsorption.[5,17] These experimental observations were confirmed by recent molecular dynamics simulations based on classical potentials for describing the interactions between the whole system.[19,20] These authors reported concerted cation motions which involved jumps between SI, SI′, SII, and SII′ sites.

Methanol, the subject of our own study, is involved in several industrially important reactions such as Mobil's methanol-to-gasoline (MTG) and methanol-to-olefin (MTO) processes.[21,22] It is also used as an alkylating agent for aromatic compounds in zeolite-catalyzed reactions.[23] This reaction takes place in a number of basic zeolites, including alkali-metal-exchanged X and Y zeolites where the extraframework cations play a crucial role by activating the methanol molecules.[24,25] A deeper understanding of the interactions between the cations and the

* To whom correspondence should be addressed. E-mail: gmaurin@lpmc.univ-montp2.fr (G.M.); rob@ri.ac.uk (R.G.B.).
† Université Montpellier II.
‡ Royal Institution of Great Britain.

10.1021/jp062059j CCC: $33.50
Published on Web 09/02/2006

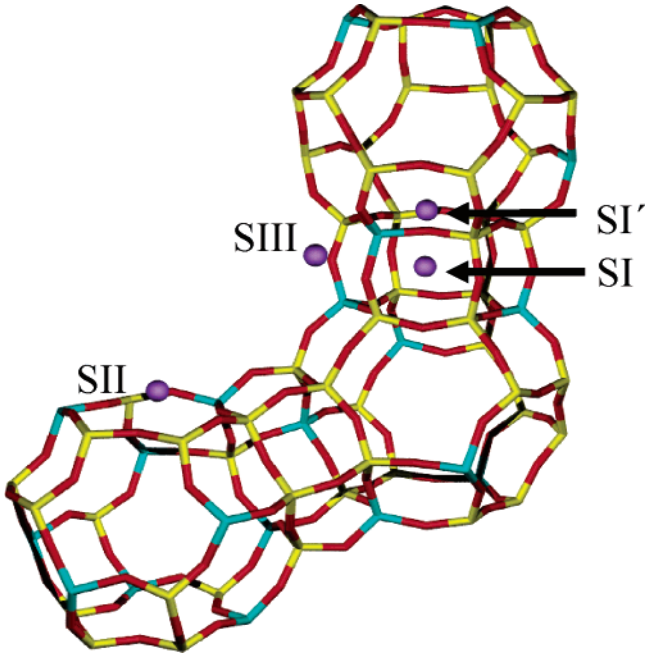

Figure 1. Molecular graphic representing the faujasite type zeolite structure with three sodalite cages connected by two hexagonal prisms. Description of the main crystallographic sites (I, I′, II, and III′) for the extraframework cations.

methanol molecules can thus provide insights into the initial stages of the alkylation reaction. In a recent study, Palomares et al.[25] carried out in situ infrared spectroscopy experiments and investigated the selective alkylation of toluene in basic zeolites as a function of the alkali cation species by studying the surface chemistry of the reactants under working conditions. Experimental results collected on Na-ZSM5, Na-MOR, or Na-FAU by temperature-programmed desorption (TPD),[26] calorimetry,[27] inelastic neutron scattering (INS),[28] and Fourier transform infrared spectroscopy (FTIR)[29] clearly show that the methanol molecules are not dissociated even at high temperatures up to 623 K, and that they strongly interact with the extraframework cations via their oxygen atoms. Here, molecular dynamics simulations were carried out to address the question of cation migration upon methanol adsorption in NaY and NaX faujasite systems as a function of the loading. Our simulations are based on our previous validated interatomic potentials[30] assuming only physisorption in the zeolite−adsorbate system. This assumption is clearly supported by the previously reported experimental data.[26−29] Simulations performed at 400 K over long simulation times allowed us to estimate both the mean square displacements (MSDs) and the (cation−methanol) radial distribution functions (RDFs) for the different types of cation sites for a wide range of loadings from 16 to 96 methanol molecules per unit cell. We are thus able to provide the cation migration mechanisms in both NaX and NaY systems and show their dependence on the adsorbate loading. The arrangement of the methanol molecules coordinated to cations located at specific sites is then compared between the two different faujasite systems.

2. Computational Methodology

Interatomic Potentials. *Zeolite Framework*. The successful simulation of cation migration upon adsorption of methanol in

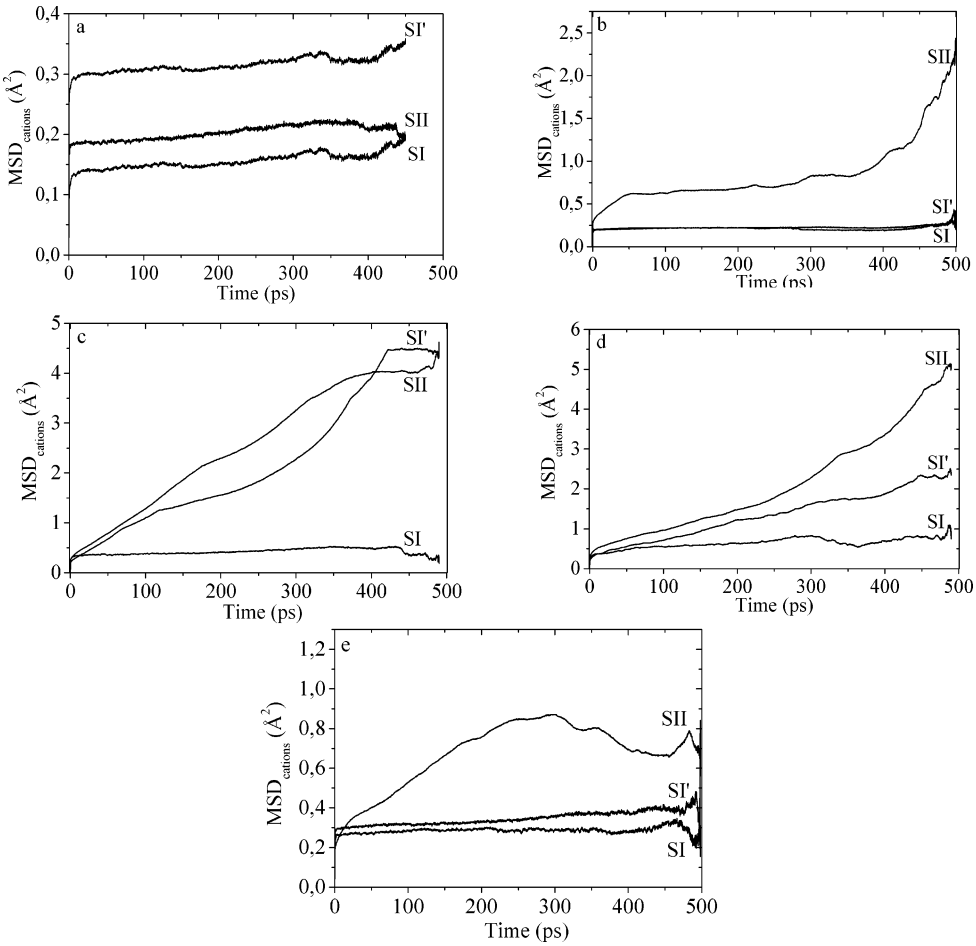

Figure 2. Mean square displacement (MSD) plots for the SI, SI′, and SII cations in NaY at 400 K and at loadings of (a) 16, (b) 32, (c) 48, (d) 64, and (e) 96 methanol molecules per unit cell.

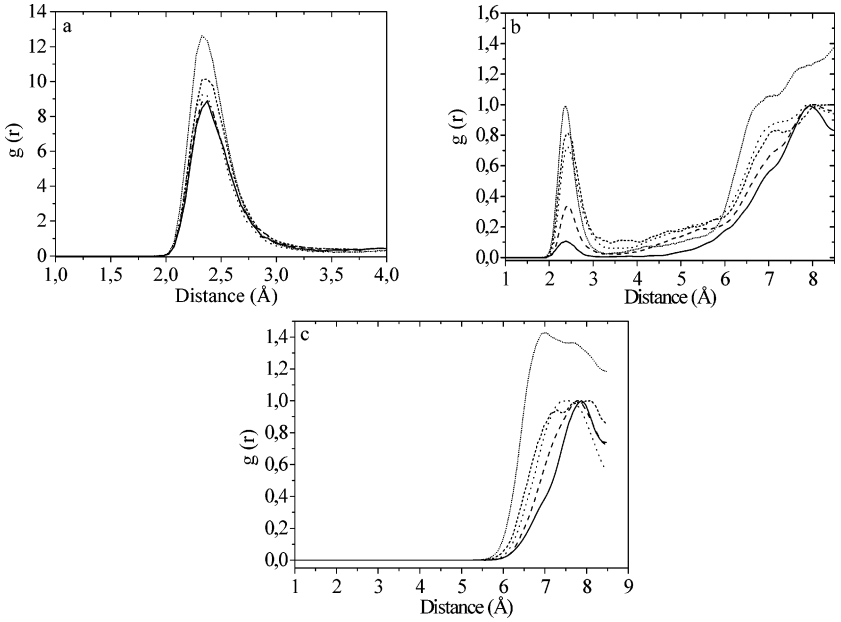

Figure 3. Radial distribution functions (RDFs) of (a) Na^+(SII)−O(methanol), (b) Na^+(SI′)−O(methanol), and (c) Na^+(SI)−O(methanol) for 16 (solid lines), 32 (dashed lines), 48 (dotted lines), 64 (short dashed lines), and 96 (short dotted lines) methanol molecules per unit cell, calculated at 400 K for the NaY−CH_3OH system.

NaX and NaY systems required an accurate description of the potential between the methanol molecules and the zeolite framework, including the sodium cations, and between the methanol molecules. Furthermore, we needed a fully flexible model in which both the zeolite and the sorbate molecules were free to alter their internal configurations. The force field used to describe the zeolite framework was selected from the work of Ramsahye and Bell[20] which includes a partially ionic model where the atoms carry the following partial charges (in electron units): Si (+2.4), Al (+1.4), O_z (−1.2), and Na (+1.0). The short-range interactions were described by Buckingham potentials, including explicit Si−O and Al−O terms, and additional harmonic three-body terms were defined for the O−Si−O and O−Al−O intratetrahedral angles.

Intermolecular Terms. Intermolecular potentials between the zeolite framework and methanol molecules are based on those reported by Blanco and Auerbach.[31] In these potentials, the short-range parts are given in the form of the Lennard-Jones 12-6 function. As we described elsewhere,[30] although the methanol partial charge distribution adopted by Blanco and Auerbach[31] accurately reproduces the dipole moment, we used different values for the atoms of the methyl group, making the C−H bonds a little more polarized, which is consistent with the ratio of charges we obtained from our previous Mulliken analysis of density functional theory (DFT) calculations.[30] For this reason, and also because of the greater ionicity of the NaY framework compared to the siliceous models (DAY and silicalite) investigated by Blanco and Auerbach,[31] the methanol-framework potential parameters were scaled slightly. The interatomic potential between methanol and the sodium cations was derived from ab initio calculations and reported in our previous paper.[30] The Lennard-Jones parameters which represent the intermolecular interactions between the methanol molecules were similarly slightly adjusted from those reported in the *cvff* force field.[32]

Methanol Intramolecular Terms. Intrasorbate flexibility was described by two-body bond stretches, three-body angle bends, and four-body torsional potentials. The corresponding parameters were obtained by slightly modifying those given by the *cvff* force field[32] in order to reproduce the experimental diffusion coefficient in the liquid phase at ambient temperature.

TABLE 1: Summed *n*(*r*) Values Calculated from the RDFs Reported in Figure 3a and b for NaY (the Integrations Are Calculated in Both Cases from 0 to 3.52 Å)

loading	$n(r)$ SII−O_m	$n(r)$ SI′−O_m
16	0.508	0.0084
32	0.936	0.0497
48	1.287	0.1618
64	1.408	0.2260
96	1.991	0.2280

All the intra- and interatomic potential parameters used are those reported in our previous paper.[30]

Zeolite Models. The crystal structures of the two faujasite systems were modeled as follows. The chemical composition $Si_{192-x}Al_xNa_xO_{384}$ was considered with $x = 92$ and $x = 56$ in order to reproduce the usual experimental Si/Al ratio for NaX and NaY, respectively. The zeolite frameworks were built in accordance with Löwenstein's Al−O−Al avoidance rule.[33] The second step consisted of modeling the distribution of the extraframework cations among the different crystallographic sites described in Figure 1. The distribution for NaY was defined as follows, based on the structure refined from X-ray diffraction data by Fitch et al:[34] 6 cations in SI sites located in the center of the hexagonal prism connecting two sodalite cages, 18 in SI′ sites in the sodalite cage in front of the 6-ring window connected to the hexagonal prism, and 32 in SII sites in the 6-ring windows of the supercages. The sites occupied were chosen randomly, with the exception that neighboring SI and SI′ sites were not allowed to be occupied. For NaX, the distribution of the extraframework cations was taken from Zhu et al.[35] with 32 Na^+ in SI′ sites, 32 Na^+ in SII sites, 28 in SIII′ sites, the two last positions corresponding to the 6-ring and 12-ring windows of the supercages, respectively. Both NaY and NaX structures were then energy minimized with the GULP code,[36] using the previously described interatomic potentials,[20] with the constraint that the cell remained cubic. These optimized structures were then loaded with 16, 32, 48, 64, and 96 methanol molecules using a canonical Monte Carlo algorithm with the sorption module implemented in the Cerius[2] program.[37] This

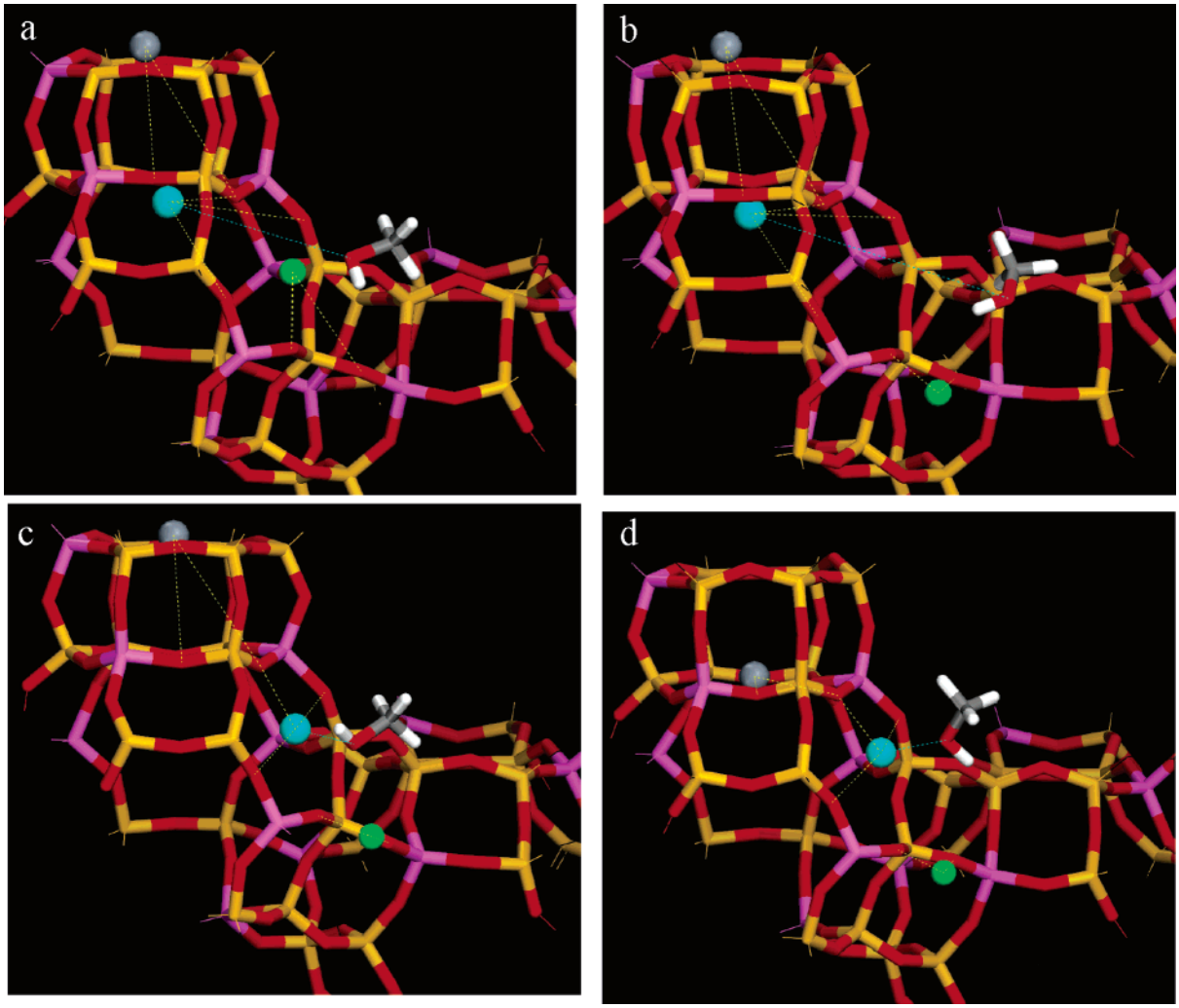

Figure 4. Typical series of images showing a concerted cation motion in NaY (loading of 48 methanol molecules per unit cell). Two SI′ and SII cations are represented in gray, light blue, and green, respectively. (a) Initial location of the cations in the two SI′ and SII sites. (b) Motion of SII cation to SIII′ site. (c) Hopping of the SI′ cation into a vacant SII position in the supercage. (d) Hopping of the second SI′ cation coming from a site within the same sodalite cages and passing through a SI site. The SII cations are represented in green.

step was simply done in order to pack molecules in and get realistic starting configurations. Furthermore, as methanol cannot access the sodalite cages, dummy atoms with appropriate van der Waals radii were placed in these cages. This was done in order to avoid any introduction of adsorbates in this space, thus leading to accessibility for gas only in the supercages. Prior to the molecular dynamics simulations, all of the structures generated were optimized using GULP where all structural parameters, that is, cell dimensions and atomic coordinates, were allowed to relax without any symmetry constraints, in order to arrive at the lowest energy starting configurations.

Molecular Dynamics Simulation. The interatomic potentials previously described for modeling the whole system were implemented in the DLPOLY program[38] in the NVT ensemble using the Evans isokinetic thermostat.[39] We selected the optimized structures obtained by the minimization procedure as starting configurations, and the minimized cell dimensions were kept fixed during the molecular dynamics (MD) runs. All components of the system (adsorbate and adsorbent) were then treated as fully flexible during the MD simulations. A time step of 1 fs was selected, with simulations run at loadings of 16, 32, 48, 64, and 96 methanol molecules per unit cell, in other words, an average of 2, 4, 6, 8, and 12 molecules per supercage, respectively. The simulations were performed at 400 K, each for 10^6 steps (i.e., 1 ns), following 50 000 steps of equilibration. A short-range cutoff of 8.50 Å was used, while electrostatic interactions were evaluated using the Ewald method. The trajectory was recorded every 200 steps during the production stage, and radial distribution functions (RDFs) were recorded every 500 steps. The mean square displacements (MSDs) of each crystallographic type of extraframework cations for each loading were evaluated by means of the following classical equation:

$$\mathrm{MSD}(t) = \langle \Delta r_j^2(t) \rangle = \frac{1}{N}\sum_{j=1}^{N} \Delta r_j^2(t) = \frac{1}{N}\sum_{j=1}^{N} (r_j(t) - r_j(0))^2 \quad (1)$$

where N corresponds to the number of extraframework cations considered in the computation of the MSD and we used multiple time origins in order to improve the statistics of the calculation. It is important to note that throughout this paper the labels SI, SI′, SII, and SIII′ for the cations refer to their location in the starting configuration and not to their position at any subsequent time.

From the RDF labeled $g(r)$ in the figures, the mean number of atoms, $n(r)$, in a shell of width Δr at distance r can be calculated by the following equation:

$$g(r) = n(r)/(\rho 4\pi r^2 \Delta r) \quad (2)$$

where ρ is the mean atom density.

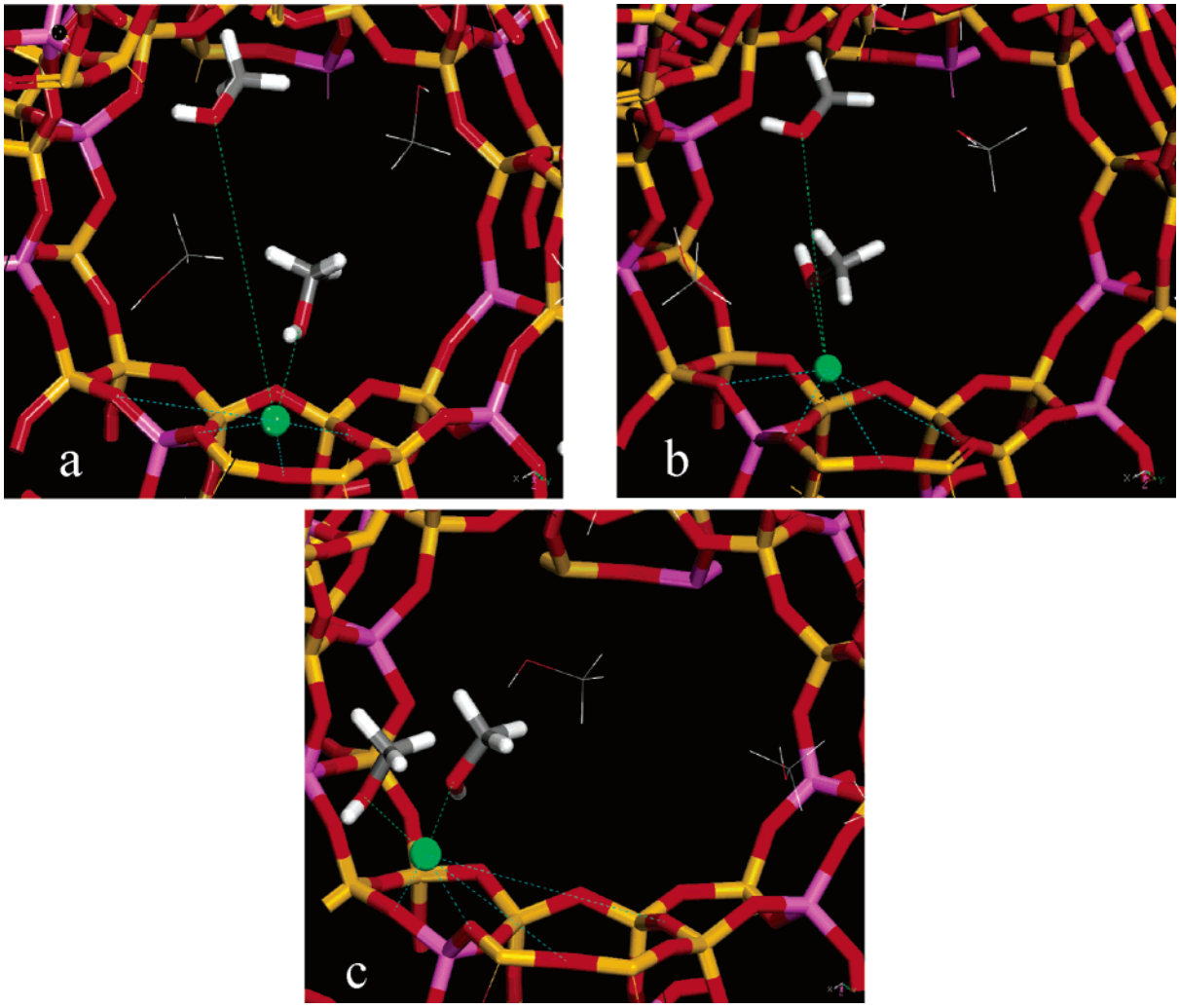

Figure 5. Typical series of images showing a single cation motion in NaY from SII (a) to SIII′ (c). Part b corresponds to an intermediate configuration between the initial and final states.

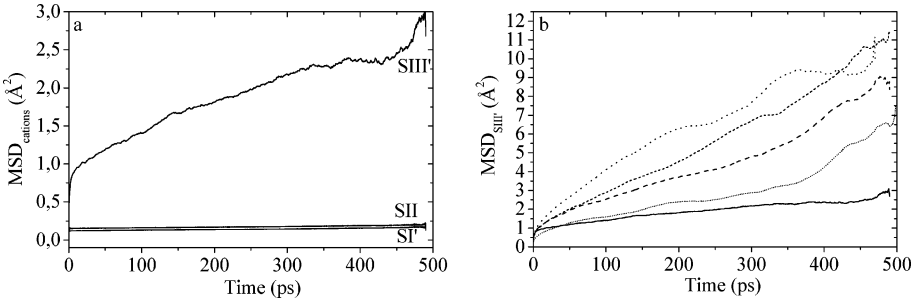

Figure 6. (a) Mean square displacement (MSD) plots for the SI′, SII, and SIII′ cations in NaX at 400 K and at a loading of 16 methanol molecules per unit cell. (b) MSD plots for the SIII′ as a function of the loading for 16 (solid lines), 32 (dashed lines), 48 (dotted lines), 64 (short dashed lines), and 96 (short dotted lines) molecules per unit cell.

3. Results and Discussion

As previously reported by Ramsahye et al.[20] using the same force field for describing the zeolite framework, the Na^+ are essentially immobile in the bare NaY and NaX at 400 K. Figure 2 shows the MSD plots for the different cation sites in NaY at the various loadings investigated (16, 32, 48, 64, and 96 methanol molecules per unit cell). At the initial stage of adsorption (Figure 2a), one can observe that the cations are not significantly displaced and the shape of the MSD plots suggests small vibrational amplitudes around their mean positions. Inspection of both of the trajectories confirm that most cations remain in their initial sites, but it also shows that a very small number of SII cations are slightly displaced due to interactions with adsorbed methanol molecules. For 32 methanol molecules per unit cell, it can be seen that some cations located in the SII site migrate from their positions toward the supercage where they are interacting with oxygen atoms near SIII′ sites and adsorbate molecules. The MSD plot reported in Figure 2b reflects this finding. This displacement is followed by the hopping of SI′ cations from the sodalite cage into the supercage to fill the vacant SII sites. A second SI′ cation can migrate across the double six ring and takes the original position of the cation that has migrated into the supercage.

This is illustrated in the RDFs for the SI′ cations and oxygen atoms of the methanol (Figure 3b) where one peak centered around 2.5 Å appears which can only be the signature of cations

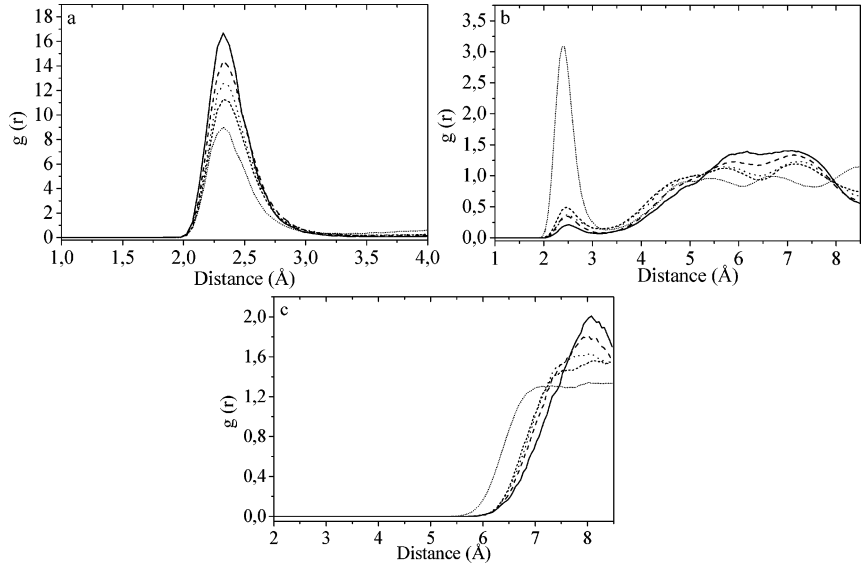

Figure 7. Radial distribution functions (RDFs) of (a) Na^+(SIII′)−O(methanol), (b) Na^+(SII)−O(methanol), and (c) Na^+(SI′)−O(methanol) for 16 (solid lines), 32 (dashed lines), 48 (dotted lines), 64 (short dashed lines), and 96 (short dotted lines) methanol molecules per unit cell, calculated at 400 K for the NaX−CH_3OH system.

interacting with the methanol molecules within the supercage as the adsorbate molecules cannot access the sodalite cages. Although this type of motion requires the cation to pass through a zeolite six ring with a high activation barrier, this result is not so surprising, as it has been already observed upon the adsorption of halocarbons with a sequence of SI′−SII′−SII hops.[16,20] At intermediate loadings (32 and 48 methanol molecules per unit cell), a larger number of SI′ and SII cations are involved in the aforementioned migration mechanism. The SII cations are characterized by motions on a large scale, as reflected by the MSD plots (Figure 2c and d), corresponding to displacement toward the center of the faujasite supercage. The resulting vacant positions are filled by migrating SI′ cations, as illustrated by the growing peak centered around 2.5 Å (Figure 3b) and the increase of the summed $n(r)$ values reported in Table 1 corresponding to the integration of this peak between 0 and 3.52 Å. Finally, at high loading (Figure 2e), SI and SI′ cations are essentially immobile and SII cations exhibit only short-range displacements due to the steric hindrance effect caused by the presence of 12 methanol molecules (on average) within the supercage. In addition, the MSD plots suggest that the SI cations are not significantly displaced during the whole adsorption process and are not involved in migration through the supercage, as it is clearly indicated by the absence of peak in the RDF (SI−oxygen of methanol) in the region 2−3 Å (Figure 3c). An illustration of these cation displacements is provided in Figure 4, obtained for the case of 48 methanol molecules per unit cell. The cations initially located in the SII site (Figure 4a) are detrapped by the presence of the adsorbate molecules and are held in a new position which is close to the SIII′ site (Figure 4b). The so-created SII vacant position promotes the migration of the SI′ cation (Figure 4c) followed by the migration across the cage of a second SI′ cation coming from a site within the same sodalite cage and passing through a SI site (Figure 4d). This type of concerted cation rearrangement may occur more frequently during a simulation over a longer time. The observation of such a cation motion sequence is consistent with recent data obtained by dielectric relaxation spectroscopy on "dry" NaY which shows that the de-trapping energy of the cation increases in the series SII > SI′ > SI.[40]

A typical single cation motion is provided in Figure 5. It is clearly shown that, first, one adsorbed methanol molecule drags the cation initially located in a SII site (Figure 5a) out of the six-ring window up to an intermediate state within the supercage (Figure 5b) before moving it to a SIII site by interacting with a second adsorbate molecule. This observation is in good agreement with the data reported in Table 1, where it is clearly shown that the extraframework cations labeled SII at the start of the simulation can coordinate up to two methanol molecules at a high loading. This result is in very good agreement with our previous studies which showed that the strong interactions between methanol oxygen and the Na^+ extraframework cation which predominantly governs the transport properties in faujasites favor the formation of adsorbate dimers coordinated to the cations.[30]

TABLE 2: Summed $n(r)$ Values Calculated from the RDFs Reported in Figure 7a and b (the Integrations Are Calculated in Both Cases from 0 to 3.22 Å)

loading	$n(r)$ SIII′−O_m	$n(r)$ SII−O_m
16	0.476	0.012
32	0.905	0.037
48	1.209	0.069
64	1.473	0.112
96	1.745	0.718

Figure 6a shows the MSD plots for the SI′, SII, and SIII′ cations in NaX at low loading (16 methanol molecules per unit cell). It can be observed that the SIII′ cations are significantly displaced, whereas SI′ and SII remain located in their initial positions. This general behavior is observed at each loading even in the case of 96 methanol molecules per unit cell. This result can be explained by the fact that the SIII′ cations are the preferential adsorption sites as confirmed by the RDFs (SIII′ cations−oxygen of methanol) (Figure 7a) and the corresponding summed $n(r)$ reported in Table 2. In this table, it is clearly shown that the coordination of SII cations between 0 and 3.22 Å is very limited up to 64 methanol molecules per unit cell compared to those obtained for the SIII′ site. The methanol molecules tend to detrap these cations more easily at accessible sites due to their lower coordination to the oxygen of the zeolite framework when compared to cations at the SII sites, leading to SIII′ cation migration toward the center of the supercage where they may be more favorably solvated by the adsorbate molecules. The MSD plot in Figure 6b shows that the mobility of the SIII′ cation is greatest for 48 methanol molecules per unit cell and then

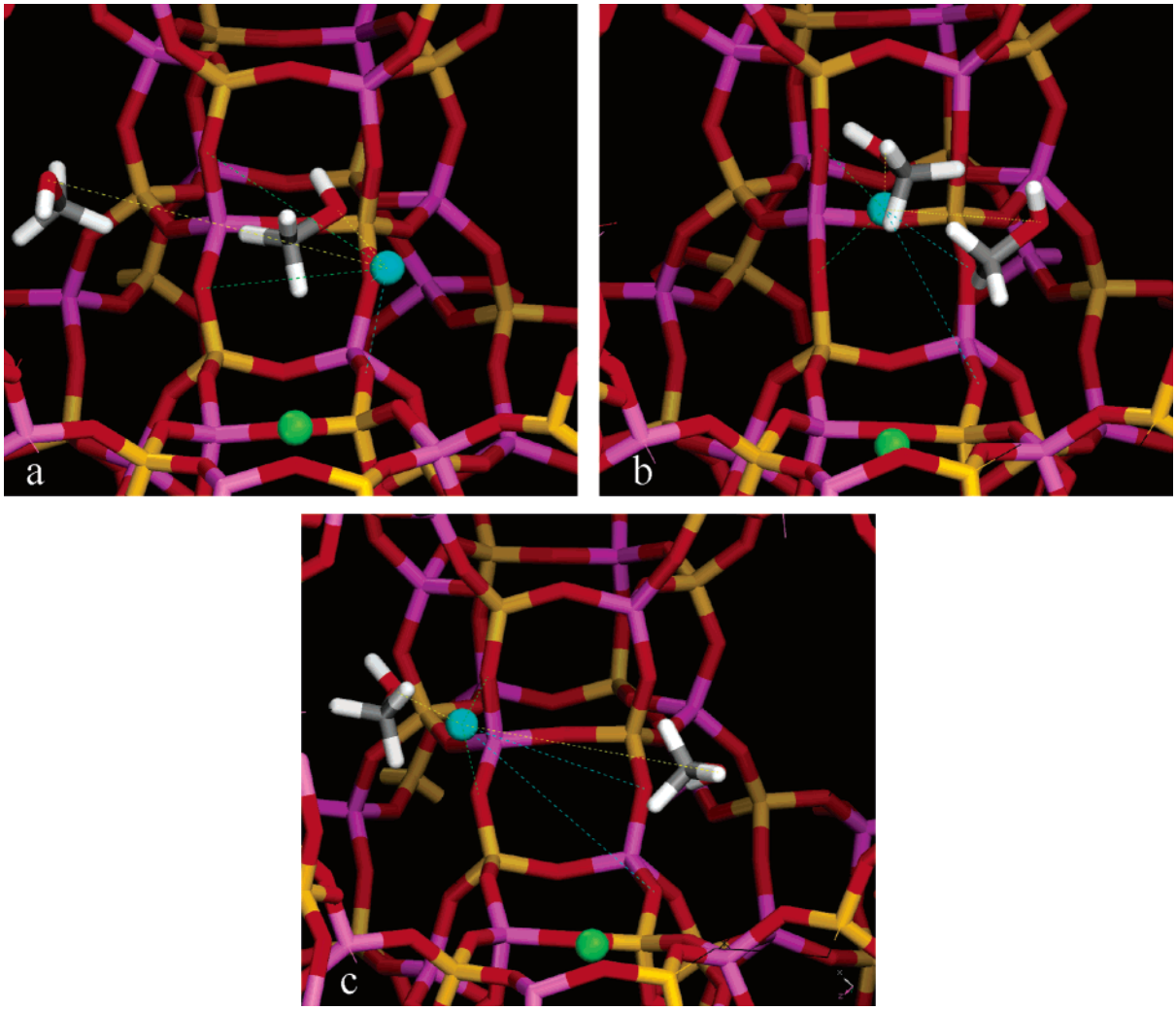

Figure 8. Typical series of images showing a single cation motion in NaX from SIII′ (a) to another SIII′ (c). Part b corresponds to an intermediate configuration between the initial and final states. The SII and SIII′ cations are represented in green and light blue, respectively.

decreases for higher loadings due to steric hindrance. It has to be mentioned that the mobility of SIII′ cations in NaX (Figure 6b) is higher than that of SII cations in NaY (Figure 2) for a given loading. In addition, the SII cations in NaX are not displaced upon the whole adsorption process even when they start to be coordinated at high loading by surrounding methanol molecules (Figure 7b, Table 2). Indeed, no vacant SII sites are available, thus avoiding the migration of SI′ cations through the six-ring windows which was previously mentioned in NaY. The RDFs (SI′ cations−oxygen of methanol) (Figure 7c) confirm this finding with the total absence of a peak in the domain of 2−3 Å. The analysis of the trajectories show that the SIII′ cations migrate out of their original positions into nearby SIII′ upon the coordination of the adsorbate molecules. A typical illustration is provided in Figure 8 where one can observe that a first methanol molecule detraps a SIII′ cation (Figure 8a), leading to an intermediate state (Figure 8b) before migrating to another SIII′ site (Figure 8c).

4. Conclusion

Molecular dynamics simulations performed on a large time scale were revealed to be a powerful tool for studying the cation redistribution upon the adsorption of methanol in NaY and NaX faujasite systems. A concerted migration mechanism has been suggested for NaY. It involves the motion of SII cations toward the center of the supercage, leading to vacant SII positions which are filled by SI′ cations diffusing through the six-ring windows. Another SI′ cation can thus migrate into the nearby SI′ free site. Single cation rearangements were also proposed, leading to displacements of SII cations to vacant SIII′ sites. The amplitude of the cation motions depends on the loading and becomes limited for the highest number of methanol molecules per unit cell. By contrast, in NaX, only the SIII′ cations are moved upon adsorption due to accessible location which makes them preferentially coordinated to the adsorbate molecules. It was thus shown that the SIII′ cations migrate out of their original positions into nearby vacant SIII′ sites. These results will be compared in the future with experimental data extracted from dielectric relaxation spectroscopy which will allow us to define the distribution of the cations within the crystallographic sites during the whole adsorption process. Furthermore, we have recently shown that the energy barriers for a sodium cation to migrate from the SI′ to SII sites decrease with increasing number of aluminum atoms in the zeolite six ring.[41] We observed a better agreement with DRS experiments for three aluminum atoms in the six ring. In our future simulations, we will probe different aluminum arrangements in the six-membered and four-membered rings which hold the SII and SIII′ cations.

Acknowledgment. We would like to thank Dr. Naseem Ramsahye for fruitful discussions.

References and Notes

(1) Gottardi, G.; Galli, E. *Natural Zeolites*; Springer-Verlag: Berlin, 1985; p 223.
(2) Van Bekkum, H., Flanigen, E. M., Jacobs, P. A., Jansens, J., Eds. *Introduction to Zeolite Science and Practice*; Studies in Surface Science and Catalysis; Elsevier: Amsterdam, The Netherlands, 2001; p 137.
(3) Demontis, P.; Suffritti, G. B. *Chem. Rev.* **1997**, *97*, 2845.
(4) Mortier, W. J. *Compilation of extra-framework Sites in Zeolites*; Butterworth: Guildford, U.K., 1982.
(5) Bosch, E.; Huber, S.; Weitkamp, J.; Knozinger, H. *Phys. Chem. Chem. Phys.* **1999**, *1*, 579.
(6) Maurin, G.; Llewellyn, P.; Poyet, T.; Kuchta, B. *J. Phys. Chem. B* **2005**, *109*, 125.
(7) Calero, S.; Dubbeldam, D.; Krishna, R.; Smit, B.; Vlugt, T. J. H.; Denayer, J. F. M.; Martens, J. A.; Maesen, T. L. M. *J. Am. Chem. Soc.* **2004**, *126*, 11377.
(8) Maurin, G.; Bell, R.; Devautour, S.; Giuntini, J. C.; Henn, F. *J. Phys. Chem. B* **2004**, *108*, 3739.
(9) Devautour, S.; Abdoulaye, A.; Giuntini, J. C.; Henn, F. *J. Phys. Chem. B* **2001**, *105*, 9297.
(10) Beauvais, C.; Boutin, A.; Fuchs, A. H. *ChemPhysChem* **2004**, *5*, 1791.
(11) Norby, P.; Poshni, F. I.; Gualtieri, A. F.; Hanson, J. C.; Grey, C. *J. Phys. Chem. B* **1998**, *102*, 839.
(12) Shirono, K.; Endo, A.; Daiguji, H. *J. Phys. Chem. B* **2005**, *109*, 3446.
(13) Pichon, C.; Palancher, H.; Lynch, J.; Hordeau, J. L.; Berar, J. F. *Stud. Surf. Sci. Catal.* **2005**, *158*, 789.
(14) Faux, D. A. *J. Phys. Chem. B* **1998**, *102*, 10658.
(15) Lee, Y.; Vogt, T.; Hriljac, J. A.; Parise, J. B.; Hanson, J. C.; Kim, S. J. *Nature* **2002**, *420*, 485.
(16) Grey, C. P.; Poshni, F. I.; Gualtieri, F.; Norby, P.; Hanson, J. C.; Corbin, D. R. *J. Am. Chem. Soc.* **1997**, *119*, 1981.
(17) Sanchez-Sanchez, M.; Blasco, T.; Rey, F. *Phys. Chem. Chem. Phys.* **1999**, *1*, 4529.
(18) Mellot-Draznieks, C.; Rodriguez-Carvajal, J.; Cox, D. E.; Cheetham, A. K. *Phys. Chem. Chem. Phys.* **2003**, *5*, 1882.
(19) Jaramillo, E.; Grey, C. P.; Auerbach, S. M. *J. Phys. Chem. B* **2001**, *105*, 12319.
(20) Ramsahye, N. A.; Bell, R. G. *J. Phys. Chem. B* **2005**, *109*, 4738.
(21) Gayubo, A. G.; Aguayo, A. T.; Atutxa, A.; Prieto, R.; Bilbao, J. *Ind. Eng. Chem. Res.* **2004**, *43*, 5042.
(22) Patca, F. C. *J. Catal.* **2005**, *231*, 194.
(23) Borgna, A.; Sepulveda, J.; Magni, S. I.; Apesteguia, C. R. *Appl. Catal., A* **2004**, *276*, 207.
(24) Wieland, W. S.; Davis, R. J.; Garces, J. M. *J. Catal.* **1998**, *173*, 490.
(25) Palomares, A. E.; Eder-Mirth, G.; Rep, M.; Lercher, J. A. *J. Catal.* **1998**, *180*, 56.
(26) Hunger, B.; Matysik, S.; Heuchel, M.; Einicke, W. D. *Langmuir* **1997**, *13*, 6249.
(27) Izmailova, S. G.; Karetina, I. V.; Khvoshchev, S.; Shubaeva, M. A. *J. Colloid Interface Sci.* **1994**, *165*, 318.
(28) Schenkel, R.; Jentys, A.; Parker, S. F.; Lercher, J. A. *J. Phys. Chem. B* **2004**, *108*, 15013.
(29) Ziolek, M.; Czyzniewska, J.; Lamotte, J.; Lavalley, J. C. *Zeolites* **1996**, *16*, 42.
(30) Plant; D. F.; Maurin, G.; Bell, R. B. *Microporous Mesoporous Mater.*, submitted for publication.
(31) Blanco, C.; Auerbach, S. M. *J. Phys. Chem. B* **2003**, *107*, 2490.
(32) Discover 2.9.7/95.0/3.0.0 User Guide; MSI:, B., Ed. San Diego, CA, 1995.
(33) Lowenstein, W. *Am. Mineral.* **1954**, *39*, 92.
(34) Fitch, A. N.; Jobic, H.; Renouprez, A. *J. Phys. Chem. B* **1986**, *90*, 1311.
(35) Zhu; L.; Seff, K. *J. Phys. Chem. B* **1999**, *103*, 9512.
(36) Gale, J. D. *J. Chem. Soc., Faraday Trans.* **1997**, *93*, 629.
(37) *Cerius2 v. 4.2*; Accelrys, Inc.: San Diego, CA, 1999.
(38) Smith, W.; Forester, T. R. *J. Mol. Graphics* **1996**, *14*, 136.
(39) Frenkel, D.; Smit, B. *Understanding Molecular Simulation*; Academic Press: San Diego, CA, 1996.
(40) Devautour, S.; et al. *J. Phys. Chem. B*, submitted for publication.
(41) Ramsahye, N. A.; et al. *Phys. Chem. Chem. Phys.*, submitted for publication.